Synthesis and characterization of peri-heptacene on a metallic surface

Kalyan Biswas, Dr. José I. Urgel, Dr. M. R. Ajayakumar, Dr. Ji Ma, Dr. Ana Sánchez-Grande, Shayan Edalatmanesh, Dr. Koen Lauwaet, Dr. Pingo Mutombo, Dr. José M. Gallego, Prof. Rodolfo Miranda, Prof. Pavel Jelínek, Prof. Xinliang Feng, Prof. David Écija

Synthesis and characterization of peri-heptacene on a metallic surface

Kalyan Biswas,[a] José I. Urgel,[a,*] M. R. Ajayakumar,[b] Ji Ma,[b] Ana Sánchez-Grande,[a] Shayan Edalatmanesh,[c,d] Koen Lauwaet,a Pingo Mutombo,[c] José M. Gallego,[e] Rodolfo Miranda,[a,f] Pavel Jelínek,[c,d,*] Xinliang Feng,[b,*] and David Écija[a,*]

[a] Kalyan Biswas, Dr. José I. Urgel, Dr. Ana Sánchez-Grande, Dr. Koen Lauwaet, Prof. Rodolfo Miranda and Prof. David Écija. IMDEA Nanoscience, C/ Faraday 9, Campus de Cantoblanco, 28049 Madrid, Spain

[b] Dr. M. R. Ajayakumar, Dr. Ji Ma and Prof. Xinliang Feng. Center for Advancing Electronics and Faculty of Chemistry and Food Chemistry, Technical University of Dresden, 01062 Dresden, Germany

[c] Shayan Edalatmanesh, Dr. Pingo Mutombo and Prof. Pavel Jelínek. Institute of Physics of the Czech Academy of Science, CZ-16253 Praha, Czech Republic

[d] Shayan Edalatmanesh and Prof. Pavel Jelínek. Regional Centre of Advanced Technologies and Materials, Palacký University Olomouc, CZ-771 46 Olomouc, Czech Republic

[e] Dr. José M. Gallego. Instituto de Ciencia de Materiales de Madrid, CSIC, Cantoblanco, 28049 Madrid, Spain

[f] Prof. Rodolfo Miranda. Departamento de Física de la Materia Condensada, Universidad Autónoma de Madrid, 28049 Madrid, Spain

Abstract: The synthesis of long n-peri-acenes (n-PAs) is challenging as a result of their inherent open-shell radical character, which arises from the presence of parallel zigzag edges beyond a certain n value. They are considered as π-electron model systems to study magnetism in graphene nanostructures; being potential candidates in the fabrication of optoelectronic and spintronic devices. Here, we report the on-surface formation of the largest pristine member of the n-PA family, i.e. peri-heptacene (n = 7, 7-PA), obtained on an Au(111) substrate under ultra-high vacuum conditions. Our high-resolution scanning tunneling microscopy investigations, complemented by theoretical simulations, provide insight into the chemical structure of this previously elusive compound. In addition, scanning tunneling spectroscopy reveals the antiferromagnetic open-shell singlet ground state of 7-PA, exhibiting singlet–triplet spin-flip inelastic excitations with an effective exchange coupling (Jeff) of 49 meV.

Over the last decade, the synthesis of structurally well-defined nanographenes (NGs), has captivated the scientific community. Such NGs can be considered as model π-electron systems in organic chemistry, with exciting properties,[1–3] which arise from their π-bond topology. The modulation of their electronic states depends heavily on the presence of parallel zigzag edges, which is typically the origin of their distinct electronic and magnetic properties, as well as their chemical reactivity.[4,5]

Among the different NG families, n-Acenes and n-peri-acenes (n-PAs) consist of linearly fused benzene rings and two laterally peri-fused linear acenes, respectively (n refers to the number of annulated rings formed along the zigzag axis), representing the two most important families of rectangle-shaped NGs. Both families can exhibit, above certain length, diradical or polyradical

character arising from the lateral π-extension of their framework by virtue of the gain of additional Clar sextets (defined as six π-electrons localized in a single benzene-like ring separated from adjacent rings by formal C–C single bonds) in their open-shell resonance forms, which may partially compensate the energy needed to dissociate a C(sp2)–C(sp2) π-bond by providing aromatic stabilization.[6,7] While the solution-based synthesis of pristine higher acenes stabilized on different matrixes has been recently achieved, they exhibit short lifetimes,[8–12] and the attachment of bulky aryl substituents onto the most reactive zigzag edges has been shown necessary to attain a reasonable kinetic stability.[13–16] In fact, by following this strategy, only recently the solution-based synthesis of 4-PA (peri-tetracene)[13,14] and 7-PA[16] employing the bulky 2,6-dichlorophenyl, mesityl and/or tert-butylphenyl groups at the reactive zigzag peripheries have been afforded.

Under this scenario, during the last decade oxidative ring-closure and cyclodehydrogenation reactions catalyzed on metal surfaces under ultra-high vacuum (UHV) conditions, have emerged as an alternative approach toward the synthesis of open-shell NGs, which could not be obtained via conventional solution synthesis. In recent years, significant progress has resulted in the synthesis and characterization, via advanced scanning probe techniques, of members of the n-acene[17–25] and triangulene[26–29] families among others.[30–34] However, only the shorter members of the n-PA family such as 2-PA (perylene),[35] 3-PA (bisanthene),[36–39] 4-PA[40]

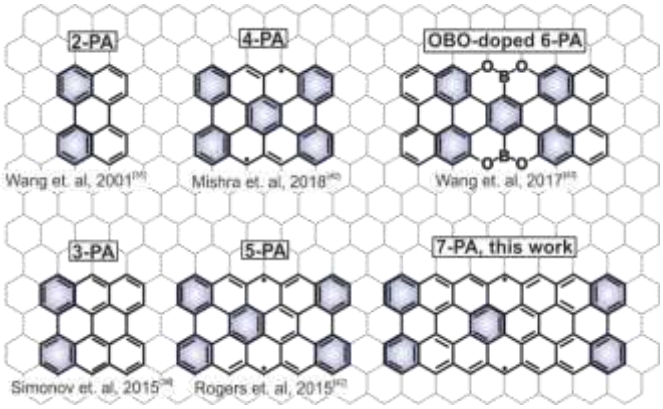

and 5-PA (peri-pentacene),[41,42] together with heteroatom-doped[43] and dibenzoperihexacene[44] derivatives, as well as several 1D carbon-based nanostructures containing n-PAs as building block units,[45–49] have been synthetized and characterized on metallic surfaces (see Scheme 1).

Scheme 1. Representative n-PA nanographenes synthesized on surfaces. 4-PA, 5-PA and 7-PA present an open-shell singlet ground state.[41,42] Their chemical sketch represents only one of the possible diradical non-Kekulé resonance structures. Purple filled benzenoid rings denote Clar sextets. The literature mentioned in the Scheme refers to the first time such compounds were studied on surfaces.

This communication presents the first synthesis, direct visualization, and electronic characterization of the longest peri-acene (7-PA) reported to date, highlighting the potential of the on-surface synthesis approach in the formation of large pristine PA species featuring increased singlet open-shell ground state character. For this purpose, we have synthesized the precursor 4,5,9,10-tetrakis(3-methylnaphthalen-2-yl)pyrene (1) in solution, which can be sublimed on Au(111) in a UHV environment and converted into the targeted 7-PA molecule by thermal activation at 300 ºC via surface-assisted oxidative ring-closure and cyclodehydrogenation reactions (Figure 1a). Our molecular-level investigations reveal the

chemical structure of 7-PA, which has been determined by scanning tunneling microscopy (STM). Furthermore, scanning tunneling spectroscopy (STS) measurements, complemented by spin-polarized density functional theory (DFT) calculations reveal the antiferromagnetic open-shell singlet ground state of 7-PA (Jeff = 49 meV). Our approach provides fundamental understanding toward the rational synthesis and characterization of NGs comprising open-shell ground states, which can also be considered as potential building blocks in the fabrication of optoelectronic and spintronic devices.

The molecular precursor 1 was synthetized in 30% yield through a Suzuki coupling reaction between compounds 4,5,9,10-tetrabromopyrene and 4,4,5,5-tetramethyl-2-(3-methylnaphthalen-2-yl)-1,3,2-dioxaborolane (see Figures S1-S3 in the Supporting Information for synthetic and characterization details). Sublimation of 1 onto a clean Au(111) surface held at room temperature and subsequent annealing to 300 °C affords the oxidative ring-closure and cyclodehydrogenation of the precursors. STM images (Figure 1b,c) reveal that approximately 8%

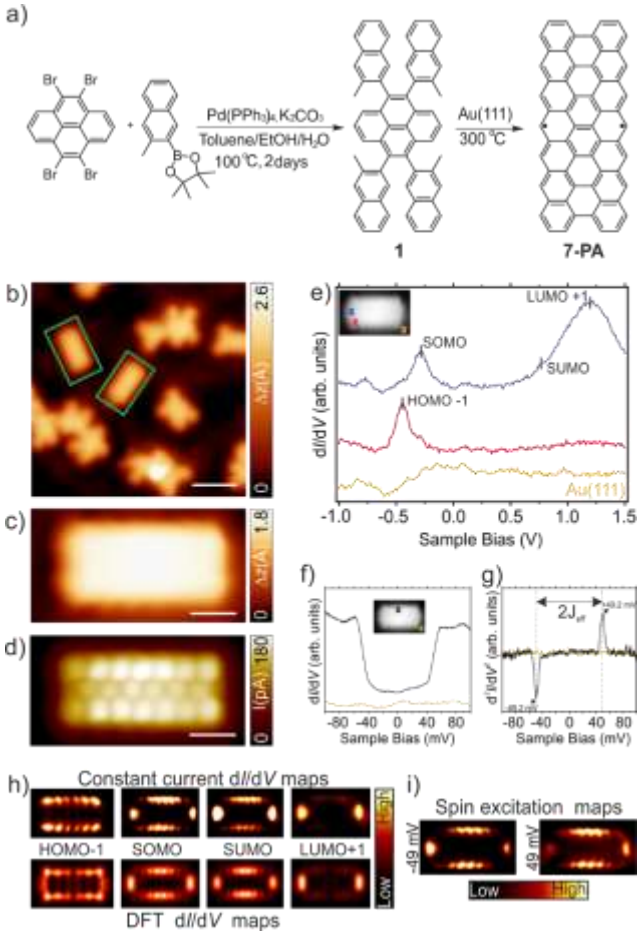

of the isolated NGs present on the surface exhibit a rectangular-shape with a uniform apparent height of 1.7 Å, which are, at this point, tentatively attributed to the formation of 7-PA. Additionally, several ill-defined NGs are formed due to loss of methyls and/or the rotation of ortho-methylnaphthalenyl substituents prior to cyclization. Such NGs coexist with fused segments which arise from the nonselective C-H bond activation that occurs at the same temperature as the formation of the expected 7-PA (see further analysis below). Constant-height STM images acquired with a CO-functionalized tip (Figure 1d) allow us to resolve features assigned to twenty benzene rings, thus directly confirming the obtained NGs as 7-PA.

Figure 1. Structural and electronic characterization of 7-PA synthetized on Au(111). a) Solution and on-surface synthesis of 7-PA reported in this work. b) Overview STM image after annealing precursor 1 at 300 °C. The green rectangles highlight two 7-PA molecules, coexisting with ill-defined nanostructures. Vb = 900 mV, It = 10 pA, scale bar 2 nm. c) High-resolution STM image of a rectangular-shaped NG assigned to a 7-PA molecule. Vb = 5 mV, It = 30 pA, scale bar 0.5 nm. d) Constant-height STM image of the same molecule acquired, resolving features assigned to twenty benzene rings (open feedback parameters: Vb = 5 mV, It = 30 pA, scale bar 0.5 nm). Both STM images shown in (c) and (d) were acquired with a CO-functionalized tip. e) Differential conductance spectra on selected positions of the 7-PA molecule; the position at which the spectrum on the molecule was acquired is highlighted in the inset STM topography image with a blue and red cross. The orange cross corresponds to the reference dI/dV spectrum acquired on Au(111). f,g) Zoomed-in differential conductance spectra (open feedback parameters, Vb = 40 mV, It = 550 pA, Vrms = 6 mV) and the corresponding inelastic electron tunnelling spectroscopy (IETS) spectra (open feedback parameters, V = 40mV, 550 pA, Vrms = 4 mV) where the value of Jeff is defined. Acquisition positions for the spectra are indicated by colour cross marks. h) Experimental dI/dV maps (top row) and calculated DFT-LDOS maps (bottom row) acquired at the HOMO-1, SOMO, SUMO and LUMO+1 resonances, respectively. Tunnelling parameters for the dI/dV maps: HOMO – 1 (Vb = −0.45 V, It = 250 pA); SOMO (Vb = −0.3 V, It = 250 pA); SUMO (Vb = 0.77 V, It = 400 pA), and LUMO + 1 (Vb = 1.20 V, It = 250 pA). Vrms = 8 mV for all the recorded spectrum and experimental maps. i) The inelastic spin excitations dI/dV maps of the 7-PA are acquired at Vb = ± 47 mV and It = 100 pA with Vrms = 10 mV.

Next, we have investigated the electronic structure of 7-PA. Spin-polarized DFT-B3LYP[50] calculations of the free-standing molecules indicate an antiferromagnetic open-shell singlet ground state (total spin S = 0), with the ferromagnetic open-shell triplet (total spin S = 1) and the nonmagnetic closed-shell states being higher in energy by 146 meV and 741 meV, respectively,[16] (see Figure S4 for the scheme of PDOS, canonical DFT orbitals for singlet open-shell structure of peri-heptacene and its spin density distribution describing the spin polarization of the molecule). In order to confirm the theoretical predictions, STS measurements are performed. Figure 1e shows the long-range differential conductance dI/dV spectra featuring a series of prominent peaks in the local density of states (LDOS) assigned to the HOMO -1 (−450 mV, HOMO = highest occupied molecular orbital), SOMO (-300 mV, SOMO = singly occupied molecular orbital), SUMO (760 mV, SUMO = singly unoccupied molecular orbital) and LUMO +1 (1200 mV, LUMO = lowest occupied molecular orbital). The experimental Coulomb gap of 7-PA is 1060 meV, established on the basis of the energies of the SOMO and SUMO resonances (110 meV smaller than the one reported for 5-PA studied on the same substrate).[41] Furthermore, a clear indication of its magnetic ground state is unveiled acquiring short-range dI/dV spectra in the proximity of the Fermi level. Figure 1f depicts such a dI/dV spectrum, which shows (respect to the Fermi level) assigned to inelastic excitation steps. Furthermore, the corresponding inelastic electron tunneling spectrum (Figure 1g) reveals an experimental exchange parameter Jeff = 49 meV (with a computed Jeff of 146 meV calculated with DFT-B3LYP, which is higher due to intrinsic limitations of the method).[41] In addition, the experimental dI/dV maps recorded at the energy position of the different frontier orbitals (Figure 1h top row) indicate a notable agreement with the calculated dI/dV maps[51,52] (Figure 1h bottom row, evaluated at a height of 4 Å above the molecular plane), further supporting our findings. The observed antiferromagnetic open-shell singlet ground state of 7-PA can be intuitively explained in terms of the Clar's sextet theory, which assumes that from the closed-shell to the open-shell diradical form, the molecule gains three aromatic sextet rings, providing extra aromatic stabilization for the open-shell ground state (Figure S5). In addition to the interplay between energy penalty for the formal loss of a π-bond and aromatic energy gain, the degeneracies of the non-Kekulé structures of 7-PA should be taken into account in order to evaluate its radical character.

Frequently, the on-surface synthesis of targeted nanostructures via oxidative ring-closure of precursors equipped with methyl groups presents several reaction pathways that hamper their

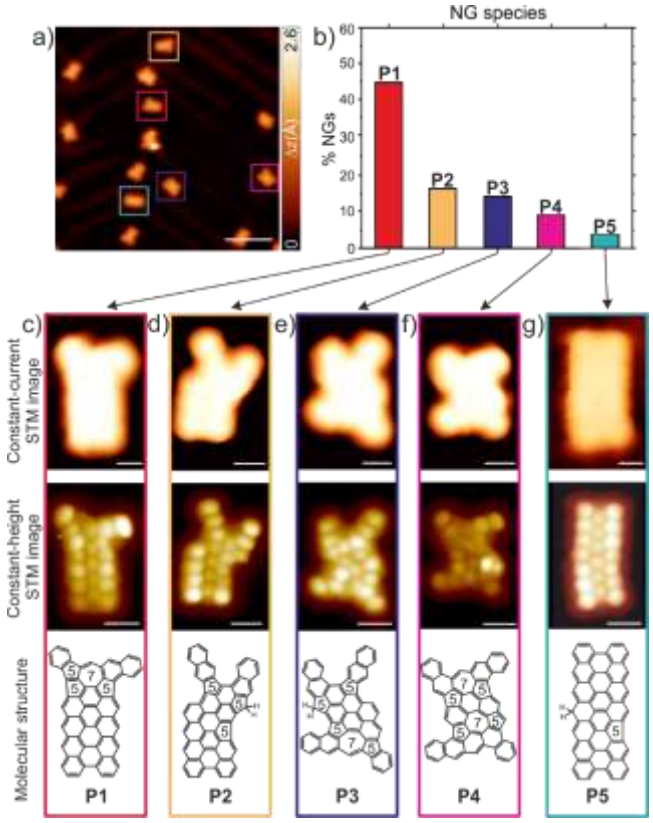

selectivity.[53–56] Therefore, in spite of the successful formation of 7-PA, we have further conducted a careful investigation of the byproducts obtained after annealing of the sample at 300 °C. Figure 2a shows a representative overview STM image where five different individual nonbenzenoid NGs (P1-P5), coexisting with a minor amount of fused species (> 5%), can be discerned. A statistical distribution of the reaction byproducts (Figure 2b, statistics over ~ 400 NGs) indicates that the majority of the NGs formed on the surface (~ 44%) present an unexpected "T-shaped" structure P1 (vertical red bar), while the formation of other asymmetrical NGs (vertical orange (P2), purple (P3), pink (P4) and light blue (P5) bars) are also observed. Such species are formed due to the cleavage of one or two methyl groups from 1 during the annealing of the sample together with the rotation of naphthalenyl units and subsequent ring rearrangement reactions as deduced from the constant-height STM images, as shown in Figure 2c-g. The possible reaction pathways towards these five byproducts are summarized in Figure S6. Finally, NGs containing saturated carbon atoms with two H atoms (those shown in Figure 2d,e,g), can be potentially transformed into fully conjugated NGs via STM tip-induced hydrogen removal, in agreement with previous reports.[26,32,40] After such manipulation, they may show prominent zero-bias peaks, attributed to a Kondo resonance (S = 1/2) (see Figure S7 for the STM tip-induced removal of a hydrogen at the saturated carbon atom of P5).[57]

Figure 2. NG species generated via loss of methyl groups prior to oxidative ring closure from 1. a) Overview STM image of the sample after annealing at 300 °C on Au(111), Vb = 500 mV, It = 30 pA, scale bar 10 nm. b) Histogram depicting the percentage of nonbenzenoid P1-P5 NGs different from 7-PA observed on the surface. c-g) High-resolution STM images of the four different byproducts (top row), bond-resolving STM images recorded with a CO-functionalized tip (middle row) and corresponding molecular structures (bottom row). The 5- and 7 membered rings in the structures are labeled for a better perception. Scanning

parameters (top row): Vb = 5 mV, It = 30 pA. Open feedback parameters (middle row): Vb = 5 mV, It = 30 pA with z-offset +70 pm, +70 pm,+ 75 pm, +60 pm and +80 pm respectively. All scale bars: 0.5 nm.

In summary, we have shown the unprecedented synthesis and characterization of the (up to now) largest member of the n-PA family, 7-PA, resulting from the oxidative ring-closure and cyclodehydrogenation reactions of precursor 1 on Au(111) upon annealing at 300 °C. The chemical structure of 7-PA has been elucidated by STM. STS measurements complemented with theoretical calculations reveal that 7-PA presents an antiferromagnetic ground state with an experimental exchange coupling of 49 meV. In addition, many of the nonbenzenoid NGs observed on the surface present a different aspect with respect to 7-PA, noticeable in the topography STM images. The formation of such NGs is attributed to the loss of one or more methyl group from 1 after annealing of the sample, which typically induces the rotation of naphthalenyl substituents followed by a ring rearrangement reaction. Our work serves as a valuable guideline for the design of new precursors toward the synthesis of open-shell NGs, shedding light on the scope and limitation of intramolecular methyl-aryl coupling. In addition, it provides new insights into the study of the n-PA family and their interesting ground states, contributing to the expansion of the chemical toolbox of organic materials with potential in semiconductor and spintronic applications.

Acknowledgements

This project has received funding from Comunidad de Madrid [projects QUIMTRONIC-CM (Y2018/NMT-4783), MAD2D, and NanoMagCost (P2018/NMT-4321)], and Ministerio de Ciencia, Innovacion y Universidades (projects SpOrQuMat (PGC2018-098613-B-C21), CTQ2017-83531-R, PID2019-108532GB-I00, and CTQ2016-81911-REDT). IMDEA Nanociencia is appreciative of support from the “Severo Ochoa” Programme for Centers of Excellence in R&D (MINECO, grant SEV-2016-0686). The EU Graphene Flagship (Graphene Core 3, 881603), ERC Consolidator Grant (T2DCP, 819698), the German Research Foundation (DFG) within the Cluster of Excellence “Center for Advancing Electronics Dresden (cfaed) and the DFG-SNSF Research Project (EnhanTopo, No. 429265950) are acknowledged for financial support. We acknowledge support from the Praemium Academie of the Academy of Science of the Czech Republic and the CzechNanoLab Research Infrastructure supported by MEYS CR (LM2018110). P.J. acknowledges the support of the GACR 20-13692X. J.I.U. acknowledges the European Union’s Horizon 2020 research and innovation programme under the Marie Skłodowska-Curie grant agreement No [886314].

References

[1] S. Song, J. Su, M. Telychko, J. Li, G. Li, Y. Li, C. Su, J. Wu, J. Lu, Chem. Soc. Rev. 2021, 50, 3238–3262.

[2] W. Zeng, J. Wu, Chem 2021, 7, 358–386.

[3] A. Narita, X.-Y. Wang, X. Feng, K. Müllen, Chem. Soc. Rev. 2015, 44, 6616–6643.

[4] J. Liu, X. Feng, Angew. Chem. Int. Ed. 2020, 59, 23386–23401.

[5] S. Fujii, T. Enoki, Acc. Chem. Res. 2013, 46, 2202–2210.

[6] T. Y. Gopalakrishna, W. Zeng, X. Lu, J. Wu, Chem. Commun. 2018, 54, 2186–2199.

[7] G. Trinquier, J.-P. Malrieu, J. Phys. Chem. A 2018, 122, 1088–1103.

[8] H. Hayashi, N. Hieda, M. Yamauchi, Y. S. Chan, N. Aratani, S. Masuo, H. Yamada, Chem. Eur. J. 2020, 26, 15079–15083.

[9] R. Mondal, R. M. Adhikari, B. K. Shah, D. C. Neckers, Org. Lett. 2007, 9, 2505–2508.

[10] R. Mondal, B. K. Shah, D. C. Neckers, J. Am. Chem. Soc. 2006, 128, 9612–9613.

[11] C. Tönshoff, H. F. Bettinger, Angew. Chem. Int. Ed. 2010, 49, 4125–4128.

[12] B. Shen, J. Tatchen, E. Sanchez-Garcia, H. F. Bettinger, Angew. Chem. Int. Ed. 2018, 57, 10506–10509.

[13] Y. Ni, T. Y. Gopalakrishna, H. Phan, T. S. Herng, S. Wu, Y. Han, J. Ding, J. Wu, Angew. Chem. Int. Ed. 2018, 130, 9845–9849.

[14] M. R. Ajayakumar, Y. Fu, J. Ma, F. Hennersdorf, H. Komber, J. J. Weigand, A. Alfonsov, A. A. Popov, R. Berger, J. Liu, K. Müllen, X. Feng, J. Am. Chem. Soc. 2018, 140, 6240–6244.

[15] J.-J. Shen, Y. Han, S. Dong, H. Phan, T. S. Herng, T. Xu, J. Ding, C. Chi, Angew. Chem. Int. Ed. 2021, 60, 4464–4469.

[16] M. R. Ajayakumar, J. Ma, A. Lucotti, K. S. Schellhammer, G. Serra, E. Dmitrieva, M. Rosenkranz, H. Komber, J. Liu, F. Ortmann, M. Tommasini, X. Feng, Angew. Chem. Int. Ed. 2021, 60, 13853–13858.

[17] J. I. Urgel, H. Hayashi, M. Di Giovannantonio, C. A. Pignedoli, S. Mishra, O. Deniz, M. Yamashita, T. Dienel, P. Ruffieux, H. Yamada, R. Fasel, J. Am. Chem. Soc. 2017, 139, 11658–11661.

[18] R. Zuzak, R. Dorel, M. Krawiec, B. Such, M. Kolmer, M. Szymonski, A. M. Echavarren, S. Godlewski, ACS Nano 2017, 11, 9321-93298.

[19] J. I. Urgel, S. Mishra, H. Hayashi, J. Wilhelm, C. A. Pignedoli, M. D. Giovannantonio, R. Widmer, M. Yamashita, N. Hieda, P. Ruffieux, H. Yamada, R. Fasel, Nat. Commun. 2019, 10, 861.

[20] J. Krüger, F. García, F. Eisenhut, D. Skidin, J. M. Alonso, E. Guitián, D. Pérez, G. Cuniberti, F. Moresco, D. Peña, Angew. Chem. Int. Ed. 2017, 56, 11945-11948.

[21] R. Zuzak, R. Dorel, M. Kolmer, M. Szymonski, S. Godlewski, A. M. Echavarren, Angew. Chem. Int. Ed. 2018, 57, 10500–10505.

[22] F. Eisenhut, T. Kühne, F. García, S. Fernández, E. Guitián, D. Pérez, G. Trinquier, G. Cuniberti, C. Joachim, D. Peña, F. Moresco, ACS Nano 2020, 14, 1011–1017.

[23] C. G. Ayani, M. Pisarra, J. I. Urgel, J. Jesús Navarro, C. Díaz, H. Hayashi, H. Yamada, F. Calleja, R. Miranda, R. Fasel, F. Martín, A. L. V. de Parga, Nanoscale Horiz. 2021, 6, 744-750.

[24] L. Colazzo, M. S. G. Mohammed, R. Dorel, P. Nita, C. G. Fernández, P. Abufager, N. Lorente, A. M. Echavarren, D. G. de Oteyza, Chem. Commun. 2018, 54, 10260–10263.

[25] M. Zugermeier, M. Gruber, M. Schmid, B. P. Klein, L. Ruppenthal, P. Müller, R. Einholz, W. Hieringer, R. Berndt, H. F. Bettinger, J. M. Gottfried, Nanoscale 2017, 9, 12461–12469.

[26] N. Pavliček, A. Mistry, Z. Majzik, N. Moll, G. Meyer, D. J. Fox, L. Gross, Nat. Nanotech. 2017, 12, 308–311.

[27] S. Mishra, D. Beyer, K. Eimre, J. Liu, R. Berger, O. Gröning, C. A. Pignedoli, K. Müllen, R. Fasel, X. Feng, P. Ruffieux, J. Am. Chem. Soc. 2019, 141, 10621–10625.

[28] J. Su, M. Telychko, P. Hu, G. Macam, P. Mutombo, H. Zhang, Y. Bao, F. Cheng, Z.-Q. Huang, Z. Qiu, S. J. R. Tan, H. Lin, P. Jelínek, F.-C. Chuang, J. Wu, J. Lu, Sci. Adv. 2019, 5, eaav7717.

[29] S. Mishra, K. Xu, K. Eimre, H. Komber, J. Ma, C. A. Pignedoli, R. Fasel, X. Feng, P. Ruffieux, Nanoscale 2021, 13, 1624–1628.

[30] S. Mishra, X. Yao, Q. Chen, K. Eimre, O. Gröning, R. Ortiz, M. Di Giovannantonio, J. C. Sancho-García, J. Fernández-Rossier, C. A. Pignedoli, K. Müllen, P. Ruffieux, A. Narita, R. Fasel, Nat. Chem. 2021, 13, 581–586.

[31] E. Turco, S. Mishra, J. Melidonie, K. Eimre, S. Obermann, C. A. Pignedoli, R. Fasel, X. Feng, P. Ruffieux, J. Phys. Chem. Lett. 2021, 12, 8314-831.

[32] T. G. Lohr, J. I. Urgel, K. Eimre, J. Liu, M. Di Giovannantonio, S. Mishra, R. Berger, P. Ruffieux, C. A. Pignedoli, R. Fasel, X. Feng, J. Am. Chem. Soc. 2020, 142, 13565–13572.

[33] J. Li, S. Sanz, J. Castro-Esteban, M. Vilas-Varela, N. Friedrich, T. Frederiksen, D. Peña, J. I. Pascual, Phys. Rev. Lett. 2020, 124, 177201.

[34] X. Su, C. Li, Q. Du, K. Tao, S. Wang, P. Yu, Nano Lett. 2020, 20, 6859–6864.

[35] D. Wang, L.-J. Wan, Q.-M. Xu, C. Wang, C.-L. Bai, Surf. Sci. 2001, 478, L320–L326.

[36] A. Ishii, A. Shiotari, Y. Sugimoto, Nanoscale 2020, 12, 6651–6657.

[37] C. Sánchez-Sánchez, T. Dienel, O. Deniz, P. Ruffieux, R. Berger, X. Feng, K. Müllen, R. Fasel, ACS Nano 2016, 10, 8006–8011.

[38] K. A. Simonov, N. A. Vinogradov, A. S. Vinogradov, A. V. Generalov, E. M. Zagrebina, G. I. Svirskiy, A. A. Cafolla, T. Carpy, J. P. Cunniffe, T. Taketsugu, A. Lyalin, N. Mårtensson, A. B. Preobrajenski, ACS Nano 2015, 9, 8997–9011.

[39] A. Jančařík, R. Zuzak, A. Jancărík, A. Gourdon, M. Szymonski, S. Godlewski, ACS Nano 2020, 14, 13316-13323.

[40] S. Mishra, T. G. Lohr, C. A. Pignedoli, J. Liu, R. Berger, J. I. Urgel, K. Müllen, X. Feng, P. Ruffieux, R. Fasel, ACS Nano 2018, 12, 11917–11927.

[41] A. Sánchez-Grande, J. I. Urgel, L. Veis, S. Edalatmanesh, J. Santos, K. Lauwaet, P. Mutombo, J. M. Gallego, J. Brabec, P. Beran, D. Nachtigallová, R. Miranda, N. Martín, P. Jelínek, D. Écija, J. Phys. Chem. Lett. 2020, 12, 330–336.

[42] C. Rogers, C. Chen, Z. Pedramrazi, A. A. Omrani, H.-Z. Tsai, H. S. Jung, S. Lin, M. F. Crommie, F. R. Fischer, Angew. Chem. Int. Ed. 2015, 54, 15143–15146.

[43] X.-Y. Wang, T. Dienel, M. Di Giovannantonio, G. B. Barin, N. Kharche, O. Deniz, J. I. Urgel, R. Widmer, S. Stolz, L. H. De Lima, M. Muntwiler, M. Tommasini, V. Meunier, P. Ruffieux, X. Feng, R. Fasel, K. Müllen, A. Narita, J. Am. Chem. Soc. 2017, 139, 4671–4674.

[44] Q. Zhong, Y. Hu, K. Niu, H. Zhang, B. Yang, D. Ebeling, J. Tschakert, T. Cheng, A. Schirmeisen, A. Narita, K. Müllen, L. Chi, J. Am. Chem. Soc. 2019, 141, 7399–7406.

[45] B. Cirera, A. Sánchez-Grande, B. de la Torre, J. Santos, S. Edalatmanesh, E. Rodríguez-Sánchez, K. Lauwaet, B. Mallada, R. Zbořil, R. Miranda, O. Gröning, P. Jelínek, N. Martín, D. Ecija, Nat. Nanotechnol. 2020, 15, 437-443.

[46] A. Sánchez-Grande, J. I. Urgel, A. Cahlík, J. Santos, S. Edalatmanesh, E. Rodríguez-Sánchez, K. Lauwaet, P. Mutombo, D. Nachtigallová, R. Nieman, H. Lischka, B. de la Torre, R. Miranda, O. Gröning, N. Martín, P. Jelínek, D. Écija, Angew. Chem. Int. Ed. 2020, 59, 17594-17599.

[47] B. de la Torre, A. Matěj, A. Sánchez-Grande, B. Cirera, B. Mallada, E. Rodríguez-Sánchez, J. Santos, J. I. Mendieta-Moreno, S. Edalatmanesh, K. Lauwaet, M. Otyepka, M. Medveď, Á. Buendía, R. Miranda, N. Martín, P. Jelínek, D. Écija, Nat. Commun. 2020, 11, 4567.

[48] X.-Y. Wang, J. I. Urgel, G. B. Barin, K. Eimre, M. Di Giovannantonio, A. Milani, M. Tommasini, C. A. Pignedoli, P. Ruffieux, X. Feng, R. Fasel, K. Müllen, A. Narita, J. Am. Chem. Soc. 2018, 140, 9104–9107.

[49] J. Li, S. Sanz, M. Corso, D. J. Choi, D. Peña, T. Frederiksen, J. I. Pascual, Nat. Commun. 2019, 10, 200.

[50] V. Blum, R. Gehrke, F. Hanke, P. Havu, V. Havu, X. Ren, K. Reuter, M. Scheffler, Comput. Phys. Commun. 2009, 180, 2175–2196.

[51] O. Krejčí, P. Hapala, M. Ondráček, P. Jelínek, Phys. Rev. B 2017, 95, 045407.

[52] P. Hapala, G. Kichin, C. Wagner, F. S. Tautz, R. Temirov, P. Jelínek, Phys. Rev. B 2014, 90, 085421.

[53] X. Xu, M. Di Giovannantonio, J. I. Urgel, C. A. Pignedoli, P. Ruffieux, K. Müllen, R. Fasel, A. Narita, Nano Res. 2021, 14, 4754-4759.

[54] S. Mishra, D. Beyer, R. Berger, J. Liu, O. Gröning, J. I. Urgel, K. Müllen, P. Ruffieux, X. Feng, R. Fasel, J. Am. Chem. Soc. 2020, 142, 1147–1152.

[55] M. Di Giovannantonio, O. Deniz, J. I. Urgel, R. Widmer, T. Dienel, S. Stolz, C. Sánchez-Sánchez, M. Muntwiler, T. Dumslaff, R. Berger, A. Narita, X. Feng, K. Müllen, P. Ruffieux, R. Fasel, ACS Nano 2018, 12, 74–81.

[56] L. Talirz, H. Söde, T. Dumslaff, S. Wang, J. R. Sanchez-Valencia, J. Liu, P. Shinde, C. A. Pignedoli, L. Liang, V. Meunier, N. C. Plumb, M. Shi, X. Feng, A. Narita, K. Müllen, R. Fasel, P. Ruffieux, ACS Nano 2017, 11, 1380–1388.

[57] M. S. G. Mohammed, L. Colazzo, R. Robles, R. Dorel, A. M. Echavarren, N. Lorente, D. G. de Oteyza, Commun. Phys. 2020, 3, 159.